

The Plasma Membrane of the Cyanobacterium *Gloeobacter violaceus* Contains Segregated Bioenergetic Domains

Sascha Rexroth,^{a,1} Conrad W. Mullineaux,^b Dorothea Ellinger,^a Esther Sendtko,^a Matthias Rögner,^a and Friederike Koenig^c

^aPlant Biochemistry, Ruhr-University Bochum, 44780 Bochum, Germany

^bSchool of Biological and Chemical Sciences, Queen Mary University of London, London E1 4NS, United Kingdom

^cMolecular Plant Physiology, University of Bremen, 28359 Bremen, Germany

The light reactions of oxygenic photosynthesis almost invariably take place in the thylakoid membranes, a highly specialized internal membrane system located in the stroma of chloroplasts and the cytoplasm of cyanobacteria. The only known exception is the primordial cyanobacterium *Gloeobacter violaceus*, which evolved before the appearance of thylakoids and harbors the photosynthetic complexes in the plasma membrane. Thus, studies on *G. violaceus* not only shed light on the evolutionary origin and the functional advantages of thylakoid membranes but also might include insights regarding thylakoid formation during chloroplast differentiation. Based on biochemical isolation and direct in vivo characterization, we report here structural and functional domains in the cytoplasmic membrane of a cyanobacterium. Although *G. violaceus* has no internal membranes, it does have localized domains with apparently specialized functions in its plasma membrane, in which both the photosynthetic and the respiratory complexes are concentrated. These bioenergetic domains can be visualized by confocal microscopy, and they can be isolated by a simple procedure. Proteomic analysis of these domains indicates their physiological function and suggests a protein sorting mechanism via interaction with membrane-intrinsic terpenoids. Based on these results, we propose specialized domains in the plasma membrane as evolutionary precursors of thylakoids.

INTRODUCTION

The appearance of eukaryotic cells is largely linked to the acquisition of cellular organelles specialized in providing energy and reducing equivalents. The establishment of chloroplasts as permanent endosymbionts constitutes a key event in the evolution of plant cells. In the chloroplast, thylakoid membranes form complicated structures known for their lateral heterogeneity. The structural complexity of thylakoids found in higher plants, with the formation of grana and stroma thylakoids, surpasses that of cyanobacterial thylakoid membranes. However, the formation of this intracellular membrane system that is entirely separated from the chloroplast inner envelope or the plasma membrane is one of the distinguishing features conserved in almost all organisms performing oxygenic photosynthesis (van de Meene et al., 2006). The cyanobacterium *Gloeobacter violaceus* (Rippka et al., 1974), the only known exception, is devoid of thylakoids. Accordingly, both the photosynthetic and the respiratory apparatus are located in its plasma membrane.

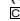
The localization of these complexes in the plasma membrane has major consequences for the protein subunits extending outward into the periplasmic region between the plasma and outer membranes (Inoue et al., 2004; Mimuro et al., 2008), as this compartment differs significantly from the environment within the thylakoid lumen. In particular, this can be recognized by the low sequence homology of the peripheral photosystem II (PSII) subunits to the sequences in other cyanobacteria (De Las Rivas et al., 2004) and by the murein binding domain found in the PsaB subunit (Grizot and Buchanan, 2004). Associated with the cytoplasmic surface of the plasma membrane is an 80-nm-thick electron-dense layer attributed to the phycobilisomes (Guglielmi et al., 1981), which, due to their bundle-shape structure, differ considerably from the hemidiscoidal shaped phycobilisomes of other cyanobacteria (Krogmann et al., 2007).

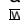
In addition to the phylogenetic analysis based on 16S rRNA (Nelissen et al., 1995) implying a divergence of *G. violaceus* prior to the endosymbiotic event in the cyanobacterial clade, there are several indications that *G. violaceus* may be considered as the most primordial cyanobacterium yet studied: This is suggested by comparative analysis with 14 other cyanobacterial genomes (Mulikidjanian et al., 2006), the lack of sulfoquinovosyl diacylglycerol (Selstam and Campbell, 1996), and a bacterial-type phytoene desaturase (Steiger et al., 2005).

Due to the uniqueness of its cellular structure, *G. violaceus* photosynthetic and respiratory complexes are restricted into a single membrane, together with the transporters, enzymes, and other components mediating the transport and biosynthetic functions of a bacterial cytoplasmic membrane. In this regard,

¹ Address correspondence to sascha.rexroth@rub.de.

The author responsible for distribution of materials integral to the findings presented in this article in accordance with the policy described in the Instructions for Authors (www.plantcell.org) is: Sascha Rexroth (sascha.rexroth@rub.de).

 Some figures in this article are displayed in color online but in black and white in the print edition.

 Online version contains Web-only data.

www.plantcell.org/cgi/doi/10.1105/tpc.111.085779

G. violaceus resembles an organism prior to the evolutionary development of the thylakoid membrane as an intracellular membrane compartment. Therefore, analyzing the cellular structure of *G. violaceus* may be valuable to define new concepts for the emergence of specialized membrane compartments and provide insights into structural and functional aspects of thylakoid formation due to the topological similarities to pro-plastids.

Membranes involved in bioenergetic processes show a high level of structural organization. Proteins and lipids, the primary constituents of biological membranes, assemble to protein complexes, such as the well-established energy conversion complexes, photosystem I (PSI), PSII, cytochrome b_6f , and ATP synthase, in the thylakoid membrane (Rexroth et al., 2003), and the higher-order structures, such as the supercomplexes (Kouril et al., 2005) or respirasomes (Schägger and Pfeiffer, 2000; Krause et al., 2004) that are formed by respiratory complexes I, III, and IV in mitochondrial membranes or the supercomplex consisting of cytochrome b_6f , PSI, and ferredoxin-NADP oxidoreductase that performs cyclic electron transport in *Chlamydomonas reinhardtii* chloroplasts (Iwai et al., 2010). Recently, a similar structural organization was also observed in bacterial systems (Lenn et al., 2008b), where oxidative phosphorylation complexes appear to be localized in segregated zones within the plasma membrane called respirazones (Lenn et al., 2008a). Segregation in biological membranes appears to be a general structural feature for the organization of cytoplasmic membranes in eukaryotic systems (Simons and Ikonen, 1997; Lingwood and Simons, 2010; Opekarová et al., 2010) but is also observed in prokaryotic systems (López and Kolter, 2010).

In this article, the occurrence of two distinct domains within the cytoplasmic membrane of *G. violaceus* was demonstrated by two independent experimental approaches. The first approach uses a simple biochemical procedure that avoids the use of any detergent to separate the two membrane domains. The second approach applies confocal microscopy to observe these two membrane domains in living cells.

Functional and structural differences of the two separated membrane domains are revealed by vast differences in their proteome and pigment composition. One domain displays characteristics of the thylakoid membranes isolated from common cyanobacteria, while the other is carotenoid rich and shows properties of a cyanobacterial plasma membrane. This separation of membrane domains correlated to their carotenoid content shows parallels to the observation of xanthophyll-rich domains in the thylakoid membrane of the high-light-adapted green alga *Dunaliella salina* (Yokthongwattana et al., 2005).

In summary, these results provide important insight into the evolution of membrane compartments in general and the biogenesis of the thylakoid membrane in particular.

RESULTS

Biochemical Separation

The primordial cyanobacterium *G. violaceus* was cultivated at light intensities of $4 \mu\text{mol photons m}^{-2} \text{s}^{-1}$ to provide stable photoautotrophic growth. For membrane isolation, cells were

harvested by centrifugation and subjected to a classical protocol (Murata and Omata, 1988) (i.e., the cells were broken by French press treatment, and sucrose density gradient centrifugation was used to separate cellular membranes). The centrifugation resulted in the separation of an orange and a green membrane fraction with densities of 1.07 and 1.16 g/mL, respectively (Figure 1). The properties of these membrane fractions in terms of protein composition, pigment content, and buoyant density are consistent with the characteristics published for cyanobacterial plasma or thylakoid membranes (Omata and Murata, 1983; Molitor and Peschek, 1986; Norling et al., 1997; Zak et al., 2001; Huang et al., 2002). They clearly differ from the properties of the outer membrane, which can be isolated at a density of 1.19 g/mL when the interface between 48 and 50% layer of the first gradient is applied to a second sucrose gradient (Figure 1D).

This result is generally observed for any cyanobacterial cell subjected to this type of analysis and is commonly attributed to the separation of thylakoid, plasma, and outer membrane. By contrast, in the case of *G. violaceus*, which is devoid of an internal thylakoid membrane system, the green and orange material originate from the plasma membrane.

Pigment Analysis

Clear differences in pigment content are observed for the two fractions. While UV/Vis spectra (Figure 2) of the green fraction display strong chlorophyll and significant phycobiliprotein absorption, the orange fraction is largely devoid of chlorophyll and phycobilisomes. In both fractions, considerable amounts of

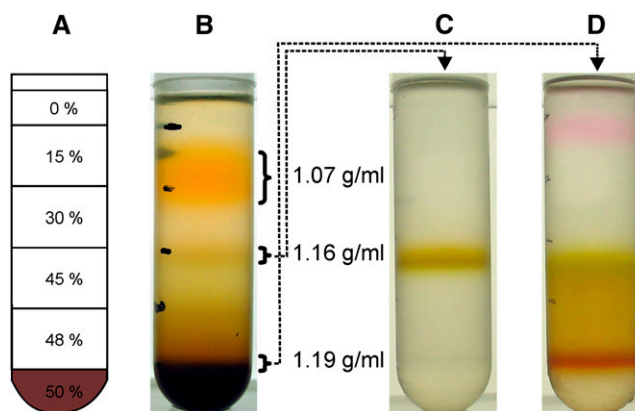


Figure 1. Sucrose Density Centrifugation of Cellular Membranes from *G. violaceus*.

(A) Schematic of the sucrose density gradients used for separation; the dark shading at the bottom represents the area of sample application in 50% sucrose (w/w).

(B) The gradient after 16 h of centrifugation at 160,000g displays an orange (1.07 g/mL) and a green (1.16 g/mL) membrane fraction.

(C) A distinct band is formed from the green fraction in **(B)** when re-centrifuged on the sucrose density gradient.

(D) A third membrane fraction with an apparent density of 1.19 g/mL (corresponding to the outer membrane) is obtained when the boundary between the 48 and 50% layer is applied to a second sucrose gradient centrifugation.

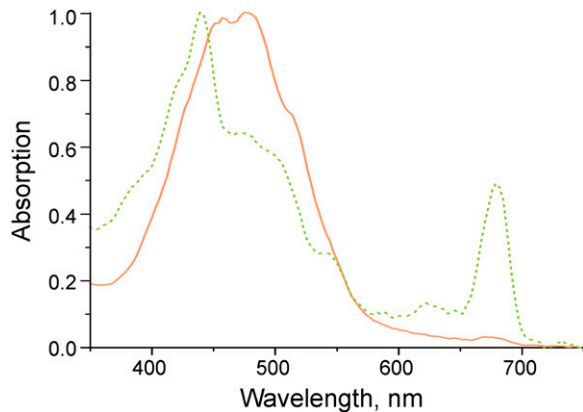


Figure 2. UV-Vis Spectra of the Isolated Membrane Fractions from *G. violaceus*.

Dotted line: the green membrane fraction from the sucrose density gradient is dominated by chlorophyll ($\lambda_{\max} = 439$ and 678 nm) absorption, with significant amounts of carotenoids ($\lambda_{\max} = \sim 450$ to 500 nm) and minor amounts of phycobilisome ($\lambda_{\max} = 625$ nm) subunits. Solid line: orange membrane fraction from sucrose density gradient containing mainly carotenoids, minor amounts of chlorophyll, and no significant absorption from phycobilisome subunits.

[See online article for color version of this figure.]

carotenoids were observed in the absorption spectra. Pronounced differences can be observed when reversed phase HPLC is employed for the separation of carotenoid species. Figure 3 shows chromatograms obtained from extracts of the orange and green membrane fraction. While all three pigments found in earlier publications (Rippka et al., 1974; Jöstingmeyer and Koenig, 1998; Tsuchiya et al., 2005), oscillaxanthin, echinenone, and β -carotene, are present in the orange fraction, the green fraction contains only echinenone and β -carotene (Table 1). Although the presence of oscillaxanthin in membranes of *G. violaceus* has been discussed (Steiger et al., 2005), both retention time and spectra (see Supplemental Figure 1 online) strongly suggest the presence of a hydrophilic carotenoid in the orange fraction. While the green membrane fraction contains 20 times more chlorophyll than the orange fraction, its carotenoid content is only 4%. Besides chlorophyll *a*, 13.2-OH chlorophyll *a* is observed by the pigment analysis as a common product of chlorophyll oxidation during extraction (Figure 3).

Lipid Analysis

As lipids play a key role in the domain formation in membranes of eukaryotic membranes, the lipid composition of both membrane fractions was characterized qualitatively and quantitatively by electrospray ionization–mass spectrometry (ESI-MS). While this analysis shows a higher content of monogalactosyldiacylglycerol (MGDG) and a lower content of digalactosyldiacylglycerol (DGDG) lipids in the orange fraction relative to the green fraction (Figure 4), these differences appear too small to induce a segregation of membrane domains. Also, length and degree of desaturation of the fatty acid substitution in the two membrane

fractions does not differ significantly (see Supplemental Figure 2 online), although the substitution pattern of MGDG and DGDG can be clearly distinguished from the phosphatidylglycerol (PG) lipids by the length and higher degree of desaturation of their fatty acid substituents. The results obtained in our investigation are in good agreement with the lipid composition published for whole *G. violaceus* cells (Selstam and Campbell, 1996).

Proteome Analysis

For characterization of the biological function, the membrane fractions were subjected to a proteome analysis based on a liquid chromatography (LC)-MS approach (Figure 5). To account for the incomplete separation of the membrane domains, the repeated occurrence of an identified protein in analytic runs of independent replicates of either the green, the orange, or both membrane fractions was required. This reduced the number of proteins passing the filter criteria set for the Sequest algorithm (Eng et al., 1994) used for protein identification criteria by 32% to 264 proteins and was a necessary step to distinguish characteristic proteins from cross-contaminants. The remaining 264 proteins were classified into three groups of proteins: those that were found either exclusively in the orange, exclusively in the green, or in both membrane fractions. While 59 of the 264 identified proteins appeared exclusively in the orange membrane fraction and 42 occurred exclusively in the green fraction, 163 were found in both fractions (Figure 5B). The high proportion of integral membrane proteins (38 and 42% identified in the orange and green fraction, respectively) indicates that both fractions indeed originate from cellular membranes and excludes soluble carotenoid binding proteins as source for the orange fraction. Table 2 contains a list of selected proteins and their occurrence in the two membrane fractions. A comprehensive list of all 264 proteins identified in the analysis can be found in Supplemental Data Set 1 online.

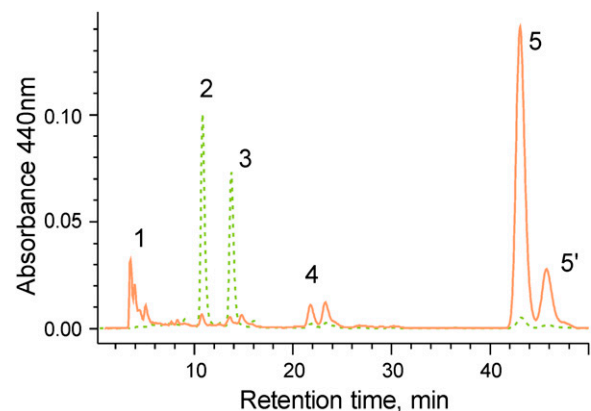


Figure 3. Pigment Analysis of the Isolated Membrane Fractions from *G. violaceus* by Reversed Phase Chromatography.

Dotted line, green membrane fraction; solid line, orange membrane fraction; 1, oscillaxanthin; 2, 13.2-OH chlorophyll *a*; 3, chlorophyll *a*; 4, echinenone; 5, β -carotene.

[See online article for color version of this figure.]

Table 1. Carotenoid Composition of the Isolated Membrane Fractions

Peak	RT (min) ^a	Orange ^b	Green ^b	Abs Max (nm)	Probable Identity ^c
1	4	0.034	–	466, 492, 524	Oscillaxanthin
2	10	0.005	0.115		13.2-OH Chlorophyll a
3	14	0.004	0.083		Chlorophyll a
4	22	0.013	0.002	~461	Echinenone
5	42	0.160	0.005	425, 448, 475	β-Carotene

^aRT, retention time.

^bAbsorbance of carotenoid and chlorophyll species estimated at 440 and 680 nm, respectively.

^cWhile there is a general agreement on the occurrence of echinenone and β-carotene (Rippka et al., 1974; Jöstingmeyer and Koenig, 1998; Tsuchiya et al., 2005), the identity of oscillaxanthin is under debate (Steiger et al., 2005).

The majority of identified proteins (163 of 264) are present in both fractions. Forty percent of these are integral membrane proteins, which in contrast with cytoplasmic matrix proteins are unlikely to be bound coincidentally as contaminants to both the orange and green membrane domains (i.e., they rather represent a significant part of the two membrane domains). Among them, identical proteins are not useful to define distinct biological functions of the two domains; however, the high number of membrane proteins shared between them is a clear indication for a common origin of the two membrane fractions.

The proteins present in both fractions represent abundant integral membrane proteins, such as the large subunits of the PSI and PSII complexes (i.e., PsaA, PsaB, D1, and D2 as well as ABC transporters). To estimate the relative amount of these proteins found in the green and orange fraction, spectral counting (Liu et al., 2004) was applied to the data obtained from the LC-MS runs. Due to its robustness when applied to membrane proteins, spectral counting, an established label-free technique for the relative quantification of protein abundance (Zybilov et al., 2006; Usaite et al., 2008), is the appropriate technique for the characterization of the complex membrane fractions obtained from *G. violaceus*. For generating an overview of the two membrane fractions (Figure 5C), normalized spectral abundance factors were employed to evaluate the distribution of proteins over categories based on the assignment in the Kyoto Encyclopedia of Genes and Genomes (KEGG) database (Kanehisa and Goto, 2000).

Proteins exclusively present in the green fraction include components of both respiratory and photosynthetic electron transport. Notably, three of the four large subunits of the cytochrome *b₆f* complex (petB, petC, and petD), five subunits of the NADH dehydrogenase complex, and five subunits of ATP synthase complex, as well as a few small subunits of the PSI and PSII complexes, are exclusively detected in the green fraction. Comparison of the relative abundance of proteins present in both fractions reveals a higher level of proteins involved in photosynthetic electron transport in the green fraction: For instance, the amount of the reaction center subunits of PSI is 5 times higher than in the orange fraction. Interestingly, the PSII core light-harvesting proteins CP43 and CP47 are 30-fold enriched in the green fraction, while the reaction center proteins D1 and D2 are only 3 times higher. The significantly higher contents of D1/D2 versus CP43/CP47 subunits indicates the absence of functional PSII complexes within the orange membranes, which is also

indicated by data from 77K fluorescence spectroscopy (see Supplemental Figure 4 online). Notably, the combination of these results is in agreement with the presence of inactive premature PSII subcomplexes as in the cytoplasmic membrane of *Synechocystis* PCC 6803 (Zak et al., 2001). In addition to subunits of the photosynthetic protein complexes, other proteins also show a clear preference for the green fraction: among them are soluble phycobilisome subunits (the α- and β-subunits of allophycocyanin, phycocyanin, and phycoerythrin) as well as cytochrome *f*, the only subunit of the cytochrome *b₆f* complex that is also detected repeatedly in the orange fraction. Within the range of error, the distribution of the photosynthetic protein complexes is consistent with the elevated chlorophyll content observed by pigment analysis.

Overall, the proteome analysis covered an extensive part of the electron transport chain. For PSII, PSI, ATP synthase, and cytochrome *b₆f*, nearly all subunits were detected in the green fraction. The only exceptions were some small subunits below 8 kD and two larger subunits, psbP of PSII and atpI of the ATP synthase (21 and 27 kD, respectively). For the NADH dehydrogenase, 10 of the 14 subunits could be identified, while subunits ndhC, ndhD, ndhE, and ndhF were not found. The extreme hydrophobicity of these proteins, ~1.0 on the GRAVY hydrophobicity scale (Kyte and Doolittle, 1982), appears not to limit the

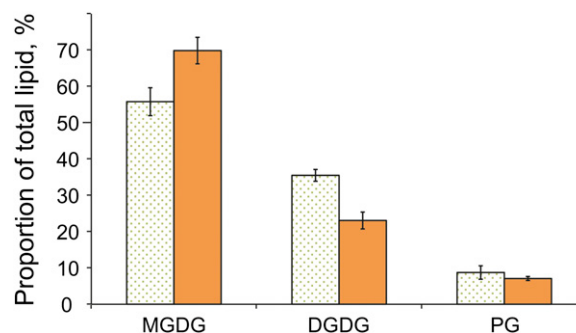


Figure 4. Distribution of Lipid Head Groups DGDG, MGDG, and PG in the Isolated Membrane Fractions from *G. violaceus* as Observed by ESI-MS.

Dotted bars, green membrane fraction; solid bars, orange membrane fraction.

[See online article for color version of this figure.]

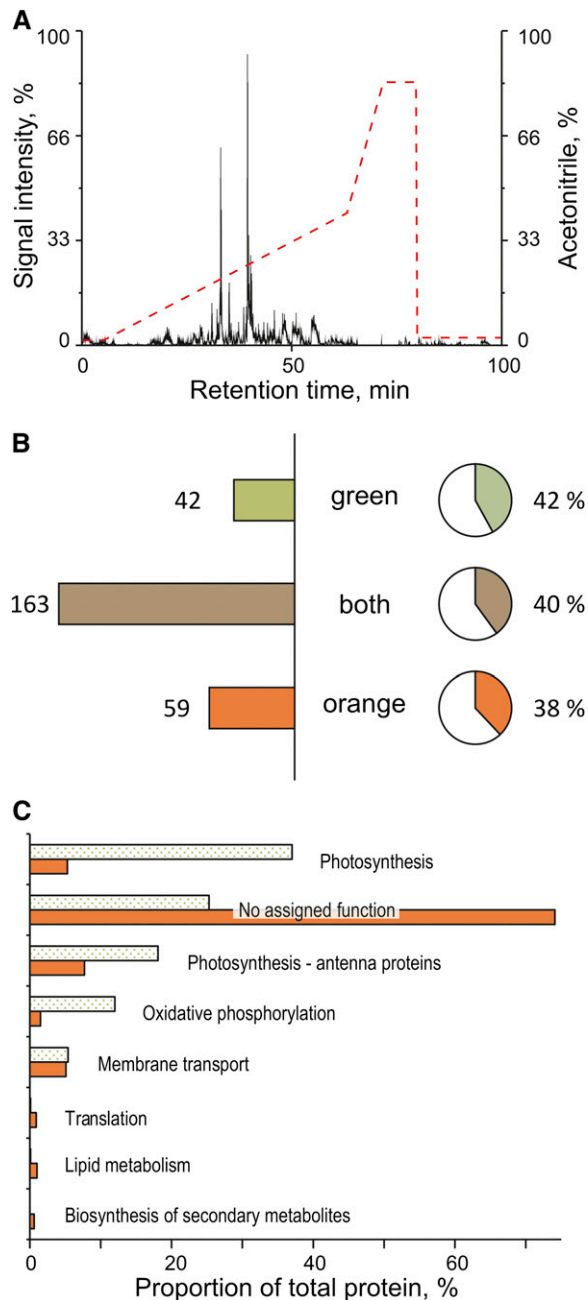


Figure 5. Summary of the Proteomic Analysis of the Two Membrane Fractions Isolated from the Cytoplasmic Membrane of *G. violaceus*.

(A) HPLC separation of tryptic peptides and applied reversed phase gradient (dotted line). The analysis is based on four analytical runs and three biological replicates for each membrane fraction.

(B) Number of proteins detected exclusively in the green, exclusively in the orange, or in both fractions (bars) and the proportion of integral membrane proteins (solid areas in circular charts) present in each of the three groups of proteins.

(C) Functional overview over the two membrane fractions based on the proteins identified. Dotted bars, green membrane fraction; solid bars, orange membrane fraction. The assignment of proteins to categories is based on the Kegg database (Kanehisa and Goto, 2000). The diagram

detection, as a number of hydrophobic proteins with similar or even higher hydrophobic indices were observed in the analysis. Subunits of the cytochrome *c* oxidase were only detected in a single LC-MS run analyzing the green membrane fraction; because we required identification in independent replicates, they were not taken into account for our analysis. However, these data suggest a low abundance of cytochrome *c* oxidase under our cultivation conditions in comparison to the other respiratory and photosynthetic protein complexes.

The group of proteins found exclusively in the orange fraction contains a significant number of enzymes involved in the metabolism of terpenoids, such as squalene-hopene cyclase, a tocopherol-cyclase homolog (*glr3089*), phytoene dehydrogenase, and cytochrome P450, but also a large amount of proteins with unknown functional assignment. Another protein significantly overrepresented in the orange fraction is a type 2 NADH dehydrogenase (*glr3503*), which is enriched by a factor of 6 relative to the green fraction. Also, a homolog of the PrtA protein, which is involved in the maturation of PSI (Klinkert et al., 2004), is exclusively located in the orange fraction.

Proteins present in both the green and the orange fraction in comparable amounts involve highly abundant membrane-associated and cytosolic proteins, like the phycobilisome core membrane linker protein *apcE* and the chaperone GroEL.

In summary, the proteomic analysis shows the presence of two distinguishable domains in the plasma membrane of *G. violaceus* originating from a single cellular membrane: one domain harbors mainly protein complexes of the photosynthetic and respiratory electron transport. The other contains accumulated carotenoids and enzymes involved in their synthesis and turnover; with the exception of a type-2 NADH dehydrogenase and a putatively functional PSI, this domain is devoid of proteins involved in electron transport.

To avoid artificial domain formation, in all experiments, the use of any detergents and organic solvents was omitted, as their effects on biological membranes are unpredictable in detail. As various other factors like temperature shifts or even counterions of charged lipids may conceivably have an impact on segregation of domains within the membrane, several control experiments have been conducted. In control experiments, a focus was set on temperature shifts as well as freezing and storage of the *G. violaceus* cells, as phase transitions in the lipid membrane were considered an important factor. However, by keeping the cells and samples during preparation at 21°C (i.e., the cultivation temperature of *G. violaceus*), we could show that temperature shifts do not influence the segregation of the domains. Furthermore, modifying pH or ion composition (from sodium to potassium) of the buffers did not have any impact on the separation (data not shown).

displays the proportion of proteins assigned to a certain category in relation to total protein amount in the respective fraction. Quantitation of proteins is based on normalized spectral counts of 222 and 205 distinct proteins for the orange and green fraction, respectively. An alternative figure displaying the absolute number of different proteins identified for the two membrane fractions is found in Supplemental Figure 3 online. [See online article for color version of this figure.]

Table 2. Relative Amount of Selected Proteins Present in the Analyzed Membrane Fractions

Protein ^a	ID ^b	Distribution ^c	Ratio ^d
Cell division protein FtsY	glr0251	Orange	–
Cobalamin biosynthesis protein CbiM	gll0292	Orange	–
DnaJ protein	glr4267	Orange	–
Phytoene dehydrogenase	glr0867	Orange	–
Shc; squalene-hopene cyclase	glr4057	Orange	–
Hypothetical protein (S-isoprenylcysteine O-methyltransferase)	gll2461	Orange	–
Hypothetical protein (tocopherol cyclase)	glr3089	Orange	–
Cytochrome P450	gll3063	Orange	–
Cytochrome P450	gll3064	Orange	–
Hypothetical protein (hopene-associated glycosyltransferase HpnB)	gll4056	Orange	–
Hypothetical protein (PrtA homolog)	glr1902	Orange	–
Hypothetical protein (YCF19)	gsr3540	Both	7.9
Hypothetical protein (steroid epimerase fam)	gll3484	Both	7.1
Probable type-2 NADH dehydrogenase	glr3503	Both	5.6
PgsA; phosphatidylglycerophosphate synthase	glr0301	Both	1.7
GAPDH	glr0530	Both	0.9
petE; plastocyanin	glr2276	Both	0.74
psbD; PSII D2	glr2323	Both	0.37
psaA; PSI, PsaA	glr3438	Both	0.27
psbA; PSII D1	glr1706	Both	0.23
petA; cytochrome f	glr3039	Both	0.16
psaB; PSI, PsaB	glr3439	Both	0.13
psbB; PSII, CP47	glr2999	Both	0.04
psbC; PSII, CP43	glr2324	Both	0.03
atpG; ATP synthase, subunit b'	gll2908	Green	–
atpH; ATP synthase, subunit c	gs12909	Green	–
petD; cyt <i>b₆f</i> , subunit 4	gll1918	Green	–
petB; cyt <i>b₆f</i> , cytochrome <i>b₆</i>	gll1919	Green	–
petC; cyt <i>b₆f</i> , Rieske subunit	glr3038	Green	–
ndhB; NDH-1, subunit 2	glr3120	Green	–
psbE, PSII, cytochrome <i>b₅₅₉</i> α	gsr0856	Green	–

^aA comprehensive table with all 265 proteins can be found in Supplemental Data Set 1 online. Homologies for hypothetical proteins detected based on amino acid sequence are denoted in parentheses.

^bAccession number as published on Cyanobase (<http://genome.kazusa.or.jp/cyanobase>).

^cObservation of identified proteins exclusively in the orange fraction, exclusively in the green fraction, or in both fractions.

^dAbundance ratio (orange/green fraction) obtained using normalized spectral abundance factors according to Zybaïlov et al. (2006). Exclusive occurrence in only one of the two fractions is denoted by a dash.

Confocal Microscopy

Although no influence of the above parameters on the separation of the membrane fractions was observed, an independent *in vivo* approach should unambiguously rule out induced artificial segregation of lipid phases. Fresh *G. violaceus* cultures with cell dimensions of ~ 1.7 by $2.5 \mu\text{m}$ were observed in their logarithmic growth phase by confocal fluorescence microscopy at 21°C (i.e., the routine growth temperature of the cells) (Figure 6). With the focal plane set at mid-cell height, the cell membranes show a halo-like appearance around the perimeter of the cell. As expected, no indications for intracellular membranes were found. Image sequences for chlorophyll (Figure 6A), phycocyanin (Figure 6B), and phycoerythrin (Figure 6C) were recorded with 3-s intervals between individual images. For all three pigments, bright patches appear in the perimeter, and these patches can be tracked in successive images. They clearly show a hetero-

geneous membrane, evidently displaying high local concentrations of photosynthetic pigments in or associated with the membrane. The fluorescent patches appear randomly distributed over the cell surface. In two-dimensional confocal optical sections, they appear as bright spots around the perimeter of the cell. Quantification of size and distribution of the fluorescent patches by images of chlorophyll fluorescence (Figure 6A) resulted in center-to-center spacing of $570 \pm 130 \text{ nm}$ ($\pm\text{SD}$). The apparent diameter of the patches was estimated for well-separated patches by extracting a line profile along the perimeter of the cell and measuring the width of the profile (full width at half maximum), resulting in a mean apparent diameter of $400 \pm 90 \text{ nm}$.

However, since the optical point spread function will be very significant at these scales, the real diameter is considerably smaller. In these images, the point spread function could be measured directly by taking line profiles perpendicular to the cell

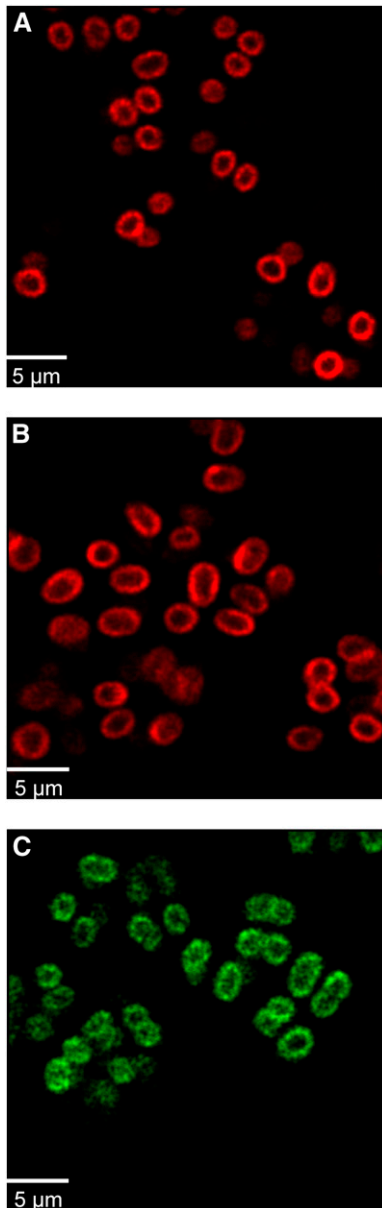


Figure 6. Confocal Fluorescence Micrographs Obtained *In Vivo* from *G. violaceus* Cultures, Showing Optical Sections in Which the Cytoplasmic Membrane Appears as a Ring around the Periphery of the Cell.

A heterogeneous distribution of fluorescence is clearly observed for chlorophyll (A), phycocyanin (B), and phycoerythrin (C). Fluorescence is concentrated in distinct spots, which display a very low diffusion rate.

perimeter, since the thickness of the membrane is negligible. These line profiles were approximately Gaussian in form, with a mean width (full width at half maximum) of 260 ± 40 nm. The real physical dimensions of the patches could then be roughly estimated by subtracting the width of the point spread function from the apparent diameter, resulting in a mean diameter (\pm SD) of 140 ± 100 nm and a mean area of $\sim 15,400$ nm². As a typical *G. violaceus* cell has a dimension of $\sim 1.7 \times 2.5$ μ m, it has a surface

area of ~ 12 μ m² (estimated by approximating the cell as a prolate spheroid). The density of the spots can be estimated from the mean center-to-center spacing as ~ 1 per 0.26 μ m². For this reason, a typical cell will contain $\sim 46 \pm 14$ fluorescent patches in its membrane, and the fluorescent patches will occupy $\sim 6\%$ of the membrane area. Figure 7 shows a model representing the dimensions and distribution of the fluorescent membrane domain in the cytoplasmic membrane of *G. violaceus*.

In summary, these results clearly show a heterogeneity of the membrane on a 100- to 200-nm scale and confirm the results from the biochemical experiments.

DISCUSSION

Separation of Membrane Domains

Analysis of membrane fractions isolated from *G. violaceus* has provided new insights into the membrane structure of this atypical cyanobacterium. Two distinct membrane fractions (a green chlorophyll-rich and a carotenoid-containing orange fraction) are obtained by applying traditional protocols for the separation of cyanobacterial membranes (Omata and Murata, 1983; Molitor and Peschek, 1986). As it is generally accepted that *G.*

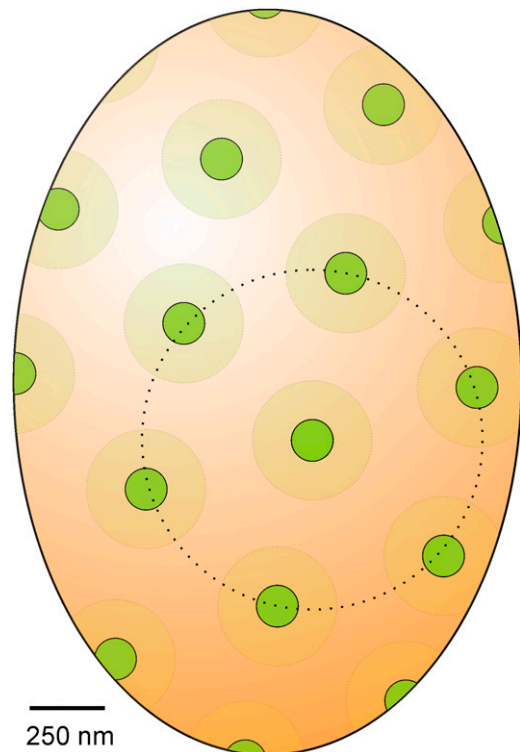


Figure 7. Membrane Domain Distribution in the Cytoplasmic Membrane of *G. violaceus* as Inferred from Confocal Microscopy.

The green domains displaying intense fluorescence emission have a mean diameter of 140 nm with a mean center-to-center distance of 570 nm (dotted line).

violaceus (Rippka et al., 1974; Guglielmi et al., 1981) contains no internal thylakoid membranes, we concluded that both membrane fractions originate from the plasma membrane and that they constitute two distinct membrane domains within this membrane.

At first sight, a preferential rupture of the membrane at the boundaries between these domains during the French press treatment (a prerequisite to facilitate the subsequent separation of the two membrane fractions) appears surprising. However, considering the fact that such domains are induced by phase separation with internal molecular interactions that have to be stronger than the interactions at the boundaries between different domains, it appears reasonable to assume such a preferential rupture. Accordingly, the boundaries between the domains should be considered as weak spots in the structural integrity of the membrane. A selective rupture of membranes at boundaries of membrane domains by mechanical force in the absence of any detergents or organic solvents was also observed for other membrane systems with lateral heterogeneity. Examples are the isolation of purple membranes from *Halobacterium salinarum* by osmotic shock (Becher and Cassim, 1975) and Y-100 stroma thylakoid particles from chloroplasts by Yeda Press (Andersson and Anderson, 1980).

Composition of the Domains

Although a perfect separation of both membrane domains cannot be expected from the applied isolation procedure, any additional purification step would inevitably introduce new potential artifacts and make the interpretation of the results more difficult and ambiguous. The restriction to the simple isolation procedure increases the robustness of the analysis, even if minor details of the domain composition remain elusive.

Based on the biochemical analysis of protein, pigment, and lipid composition of the two membrane fractions, the segregation of the membrane domains is determined by proteins and pigments, while the lipid composition seems to play a minor role. This is in contrast with the situation in lipid rafts (Simons and Ikonen, 1997) where lipid composition is the driving force for formation of microdomains.

The distribution of proteins between the two membrane domains of *G. violaceus* resembles the distribution of membrane proteins between plasma and thylakoid membrane in other cyanobacteria (Norling et al., 1997; Zak et al., 2001; Huang et al., 2002). In particular, the exclusive localization of NADH dehydrogenase (Ohkawa et al., 2001; Zhang et al., 2004) and cytochrome *b₆f* complexes (Aldridge et al., 2008; Schultze et al., 2009) in the thylakoid membrane (and their absence from the plasma membrane) has been shown for the cyanobacterium *Synechocystis* PCC 6803. This agrees well with the restriction of components from photosynthetic and respiratory electron transport chain to the green fraction. However, this is in contrast with the presence of respiratory complexes in the plasma membrane reported for other cyanobacterial species (Peschek et al., 1994), although, from an evolutionary point of view, similarities should be expected. Corresponding to the situation in *Synechocystis* PCC 6803, in the orange fraction, only PSI and a type 2 NADH dehydrogenase (Pisareva et al., 2007) are present as components of an electron transport chain, while the presence of the

PSII subunits D1 and D2 (and minor amounts of the subunits CP47 and CP43) was explained by the biogenesis of PSII (Zak et al., 2001). The exclusive location of a homolog of the PrtA protein (Klinkert et al., 2004) mediating the processing of the PSII D1 subunit in the orange fraction supports this interpretation.

Evidence for Membrane Domains in Living Cells

Confocal fluorescence microscopy of living *G. violaceus* cells confirmed the heterogeneous distribution of the three photosynthetic pigments chlorophyll, phycocyanin, and phycoerythrin within the cells. These photosynthetic pigments form patches with diameters of $\sim 140 \pm 100$ nm, which are apparent by their strong fluorescence emission. Interestingly, these dimensions are within the order of magnitude reported for lipid rafts in eukaryotic systems, ranging from <70 to 300 nm (Munro, 2003; Eggeling et al., 2009). However, they are significantly smaller than grana membranes in higher plant thylakoids with diameters of 300 to 500 nm (Mehta et al., 1999; Kaftan et al., 2002; Staehelin, 2003; Shimoni et al., 2005).

Coincidentally, the dimensions of the heterogeneous structures in the plasma membrane of *G. violaceus* match the estimated size of patches enriched in cytochrome *bd-I* complexes in *Escherichia coli* (Lenn et al., 2008b) quite well. However, a striking difference between both systems is the small diffusion rate observed for the patches in *G. violaceus*, which may be due to the murein binding domain in the PsaB subunit of *G. violaceus* (Grizot and Buchanan, 2004).

Based on size and center-to-center distances of the fluorescent patches, $\sim 6\%$ of the total membrane surface appears to be covered with the bioenergetically active patches. The comparatively small amount of these patches, which are enriched in photosynthetic pigments, is confirmed by the density gradient centrifugation (Figure 1). The fact that the chlorophyll band is faint compared with the orange band is a striking difference compared with common cyanobacteria, in which the bioenergetically active thylakoid membrane predominates. For instance, electron micrographs of low-light grown cells of *Synechococcus* sp PCC 7942 (Mullineaux and Sarcina, 2002) suggest that thylakoids constitute ~ 80 to 90% of the total membrane area (thylakoid plus cytoplasmic membrane). As no hints for heterotrophy in *G. violaceus* have been observed, the small content of membrane domains with bioenergetic activity appears to be correlated to its slow growth. It might be this slow growth lifestyle that gives *G. violaceus* the selective advantage over more evolved photoautotrophic organisms in its nutrient-poor habitat.

The fluorescent patches can be directly linked to the biochemically isolated green membrane fraction containing the vast majority of fluorescent photosynthetic pigments. While the formation of photosynthetic patches is unambiguous, a localization of the orange membrane fraction is difficult due to the lack of fluorescent pigments. Also, introducing fluorescent protein tags is unpredictable and extremely time-consuming due to the long doubling time (17 d) of *G. violaceus*. On the other hand, assignment to the dark nonfluorescent part of the cell is quite evident and consistent with the proteomic analysis: Due to the high number of membrane proteins shared between both fractions, a common origin of the green and orange membrane fractions is very likely.

Functional Implications of Membrane Segregation

The formation of stabilized membrane regions with decreased membrane fluidity in *G. violaceus* may have functional implications as membrane regions with photosynthetic complexes are separated from regions involved in biogenesis, turnover, and repair of membrane protein complexes. Also, the orange domains seem to be enriched in carotenoids, in other terpenoids, and in the proteins involved in their synthesis, processing, and turnover. As these orange membranes are largely devoid of functional photosynthetic protein complexes, they are accessible from the cytosol. This facilitates the approach of ribosomes to the membrane surface, which in turn is necessary for the co-translational insertion of membrane proteins into the membrane. The existence of defined regions for the preferential insertion of newly synthesized membrane proteins in turn supports the formation of protein complexes due to the increased local concentration of protein subunits.

From an evolutionary perspective, chloroplasts share several properties with cyanobacteria: Thylakoid membranes from chloroplasts of higher plants show a similar lipid composition with a high proportion of galactolipids containing unsaturated fatty acids. In consequence, the thylakoid membrane is a relatively fluid system (Gounaris and Barber, 1983) in comparison to other biological membranes. This membrane contains no cholesterol or other readily detectable sterols (Benson, 1964). Besides their essential function in oxidative stress, terpenoids, such as α -tocopherol (Trebst et al., 2002), and carotenoids (Demmig-Adams and Adams, 1996) help to regulate the fluidity of thylakoid membranes (Fryer, 1992; Havaux, 1998). This is evident from the zeaxanthin-related heat tolerance of thylakoids in intact leaves of higher plants (Havaux et al., 1996; Tardy and Havaux, 1997). Carotenoids that are substituted with polar groups decrease the membrane fluidity by a rivet-like mechanism due to their well-defined orientation almost perpendicular to the membrane (Subczynski et al., 1992); in this case, their polar substituents are anchored in the two opposite polar regions of the membrane. Structural significance of xanthophylls is suggested by the isolation of a xanthophyll-rich fraction from the thylakoid membrane of the high-light-adapted green algae *D. salina* (Yokthongwattana et al., 2005). Segregation of membrane compartments involved in biosynthesis of isoprenoids and photosynthetic electron transport is also observed in chloroplasts of higher plants. Besides the carotenoid transformations in the xanthophyll cycle, the synthesis of carotenoids has been shown to be restricted to the inner chloroplast envelope (Joyard et al., 2009).

Mechanism of Membrane Domain Segregation

Besides the different content of photosynthetic and respiratory protein complexes, the two domains are also very different in their carotenoid composition. Notably, the high carotenoid concentration in the orange fraction is paralleled by an increased amount of enzymes involved in the metabolism of carotenoids and other terpenoids. The preferential localization of both carotenoid-processing enzymes and their substrates might indicate a self-organizing mechanism in which release of carotenoids into the membrane induces the recruitment of carotenoid processing

enzymes nearby. Proteins and components with affinity to carotenoids will preferentially be localized in this area.

Since phase separation between membrane domains often correlates with regions of varying membrane curvature (Jülicher and Lipowsky, 1993; Parthasarathy et al., 2006), the segregation of such domains with distinct molecular composition might be sufficient to induce slight invagination or budding of membrane regions. This might be supported by differences in the preferred curvature of the components forming the membrane (Fan et al., 2010).

Evolutionarily, the segregation of functionally distinct membrane domains with well-defined protein content must precede the formation of specialized vesicles. Consequently, the initial preformation of membrane patches with protein complexes mediating photosynthetic and respiratory functions within the cytoplasmic membrane of a primitive cyanobacterium is a prerequisite for the emergence of a specialized thylakoid compartment.

In the future, analysis of unusual photoautotrophic organisms like *G. violaceus* should provide new insights into sorting mechanisms and selective transport processes, which are too complex to be easily observed in more developed plant systems.

METHODS

Culture Conditions

Gloeobacter violaceus SAG 7.82 (corresponding to PCC 7421, ATCC 29082) was cultivated photoautotrophically in Allen's medium (Allen, 1968) as 600-mL cultures in continuous white light (4 μ mol photons $m^{-2} s^{-1}$) at 21°C and was shaken by hand once per day. Cells were harvested after 6 months at culture densities of $\sim 10^8$ cells/mL, while still in the exponential growth phase, by centrifugation at 10,000g at 20°C for 10 min. The pellet was resuspended in Allen's medium with 15% (w/w) glycerol, frozen in liquid nitrogen, and stored up to two months at $-80^\circ C$. In control experiments, the freezing step was omitted and cells were processed directly without any freezing.

Isolation of Membrane Fractions

Cell disruption and separation of membrane fractions was performed by French press treatment and density gradient centrifugation according to Omata and Murata (1983) with slight modifications. For the French press treatment, a pressure of $1.2 \cdot 10^8$ Pa was applied to a cell suspension at a density of $1.5 \cdot 10^{10}$ cells/mL in BEK buffer (10 mM borate, 10 mM EDTA, and 10 mM potassium chloride, adjusted to pH 9.5 with KOH) at 4°C. Unbroken cells were removed by centrifugation (25,000g, 10 min, 4°C). Subsequently, cytoplasmic membranes were sedimented by centrifugation (150,000g, 45 min, 4°C), resuspended in BEK buffer containing 50% (w/w) sucrose, and applied at the bottom of a sucrose density step gradient with concentrations (w/w) of 40, 30, 20, 10, and 0% sucrose (Figure 1A). Centrifugation was performed in a swinging bucket rotor at 160,000g and 4°C for 16 h (Omata and Murata, 1983). Membrane fractions were removed from the gradient and stored at $-80^\circ C$. Refractometry was applied to estimate the density of the isolated fractions based on their sucrose content. In control experiments, the BEK buffer was replaced by HEN buffer (20 mM HEPES, 10 mM EDTA, and 5 mM NaCl, adjusted to pH 7.4 with NaOH) or, alternatively, the temperature was kept to 21°C to avoid freezing of the samples during harvest, cell disruption, and membrane separation.

Proteome Analysis

Fractionated membrane samples containing 100 μ g protein were digested overnight with trypsin (Promega) in solution (Blonder et al., 2006)

at a trypsin to protein ration of 1:100. Subsequent to trypsin treatment, peptides were collected and the remaining material was further incubated with both trypsin and chymotrypsin in 60% methanol for 6 h (Fischer and Poetsch, 2006). Lyophilized peptide samples from both digestion steps were dissolved in 20 μ L buffer A (95% water, 5% acetonitrile, and 0.1% formic acid) and analyzed on a 12-cm analytical C18 column (ID 100 μ m; Phenomenex Luna, 3 μ m, C18) with a 5- μ m emitter tip. For reversed phase chromatography, a linear gradient of 120 min from buffer B (10% water, 85% acetonitrile, 5% isopropanol, and 0.1% formic acid) to buffer A (95% water, 5% acetonitrile, and 0.1% formic acid) was used with a flow rate of 200 nL/min (Thermo Accela; Thermo Fisher Scientific). An online coupled Thermo LTQ Orbitrap mass spectrometer was operated in duty cycle consisting of one 300 to 2000 m/z FTMS and four MS-MS LTQ scans. Sequest algorithm (Eng et al., 1994) implemented in the Bioworks 3.3.1 software (Thermo Scientific) was applied for peptide identification versus the protein database derived from the *G. violaceus* genome sequence (Nakamura et al., 2003). False discovery rates were estimated by the number of spectral matches to a decoy database (Käll et al., 2008). Acceptance criteria and filters were set to achieve a false positive rate of <5%. Four independent samples of each membrane fraction originating from three independent biological replicates were used for the analysis. Spectral counting was used as a parameter for protein abundance (Liu et al., 2004). Normalized spectral abundance factors were calculated (Zybailov et al., 2006) for the estimation of relative differences in protein abundance (Usaitė et al., 2008; Zybailov et al., 2008; Zhang et al., 2009). Functional categories were assigned to the identified proteins based on the assignments in the KEGG database (Kanehisa and Goto, 2000).

Pigment Analysis

Reversed phase chromatography coupled to a diode array detector was used for pigment analysis as published previously (Patzlaff and Barry, 1996). Samples containing 100 μ g protein were extracted with 20% methanol in acetone under sonication (Elmasonic S 30; Elma Ultrasonic) at 4°C. The extracts were separated on a C18 column (Sperisorb ODS-2; Macherey and Nagel) applying an isocratic flow of methanol. Chromatographic traces at 440 and 665 nm were used for the estimation of carotenoid and chlorophyll contents, respectively, applying extinction coefficients of 136,400 M⁻¹ cm⁻¹ (Craft and Soares, 1992) and 71,430 M⁻¹ cm⁻¹ (Porra et al., 1989), respectively.

Lipid Extraction and Analysis

Lipids were extracted from separated membranes according to the method of Bligh and Dyer (1959). One part of extract was used for analysis of MGDG and DGDG after dilution with a solvent mixture with a final composition of chloroform:methanol:50 mM sodium acetate in water. For sulfoquinovosyl diacylglycerol and PG analysis, the extract was used after dilution in a solvent mixture with a final composition of chloroform:methanol:300 mM ammonium acetate in water. Lipids were analyzed by ESI-MS/MS after direct infusion of 5 μ L/min into a triple quadrupole tandem mass spectrometer (TSQ Vantage; Thermo). Prior to analysis, standards for MGDG and DGDG (Matreya) as well as PG (Laurodan) were added. The precursors of lipid head group-derived fragments were detected using the selected reaction monitoring scans adapted from the settings listed by Welti et al. (2002, 2003).

Confocal Microscopy

Cell suspensions were spotted onto agar plates (1.5% Bacto-Agar in growth medium), and the excess liquid was allowed to dry and absorb. Small blocks of agar with cells were then cut out and placed in a custom-built temperature-controlled sample holder with a glass cover slip on top

(Mullineaux and Sarcina, 2002). All measurements were performed at 21°C. Cells were imaged with a confocal laser scanning microscope (Nikon PCM2000) using a $\times 60$ oil immersion objective. A 20- μ m confocal pinhole was used, giving a point spread in the Z-direction of ~ 1.3 μ m (full width at half maximum). Chlorophyll fluorescence was imaged by exciting with the 488-nm line of an argon laser (Spectra-Physics), with emission defined by a Schott RG665 red-glass filter transmitting wavelengths longer than 665 nm. Phycoerythrin fluorescence was imaged by exciting with a 543-nm green helium-neon laser, with emission defined by an interference band-pass filter transmitting between 590 and 618 nm. Phycocyanin was imaged by exciting with a 633-nm red helium-neon laser, with emission defined by a 650-nm long-pass interference filter. Measurements were performed on the images and line profiles extracted using Scion Image software. For measurement of the point spread function, Gaussian curves were fitted to the line profiles using SigmaPlot 10.0 (Systat Software).

Supplemental Data

The following materials are available in the online version of this article.

Supplemental Figure 1. UV Spectra of the Hydrophilic Carotenoid Eluted from Reversed Phase Chromatography with a Retention Time of 4 min.

Supplemental Figure 2. Lipid Species Distribution for the Different Head Groups in the Isolated Membrane Fractions from *G. violaceus* as Observed by ESI-MS.

Supplemental Figure 3. Absolute Number of Different Proteins Identified and Assigned to Functional Categories.

Supplemental Figure 4. 77K Fluorescence Spectra from Isolated Membrane Fractions of *G. violaceus* Obtained by Chlorophyll Excitation at 440 nm.

Supplemental Data Set 1. Data Set of the Proteome Analysis.

ACKNOWLEDGMENTS

This article is dedicated to A. Trebst on the occasion of his 81st birthday. We thank Annette Hintelmann for her technical assistance. We acknowledge the financial support of SFB480 project C1, the Protein Research Department of the Ruhr-University Bochum project A.2.2, and the Research Development Fund of the Ruhr-University Bochum.

Received April 1, 2011; revised April 1, 2011; accepted May 14, 2011; published June 3, 2011.

REFERENCES

- Aldridge, C., Spence, E., Kirkilionis, M.A., Frigerio, L., and Robinson, C.** (2008). Tat-dependent targeting of Rieske iron-sulphur proteins to both the plasma and thylakoid membranes in the cyanobacterium *Synechocystis* PCC6803. *Mol. Microbiol.* **70**: 140–150.
- Allen, M.M.** (1968). Simple conditions for growth of unicellular blue-green algae on plates. *J. Phycol.* **4**: 1–8.
- Andersson, B., and Anderson, J.M.** (1980). Lateral heterogeneity in the distribution of chlorophyll-protein complexes of the thylakoid membranes of spinach chloroplasts. *Biochim. Biophys. Acta* **593**: 427–440.
- Becher, B.M., and Cassim, J.Y.** (1975). Improved isolation procedures for the purple membrane of *Halobacterium halobium*. *Prep. Biochem.* **5**: 161–178.

- Benson, A.A. (1964). Plant membrane lipids. *Annu. Rev. Plant Physiol.* **15**: 1–16.
- Bligh, E.G., and Dyer, W.J. (1959). A rapid method of total lipid extraction and purification. *Can. J. Biochem. Physiol.* **37**: 911–917.
- Blonder, J., Chan, K.C., Issaq, H.J., and Veenstra, T.D. (2006). Identification of membrane proteins from mammalian cell/tissue using methanol-facilitated solubilization and tryptic digestion coupled with 2D-LC-MS/MS. *Nat. Protoc.* **1**: 2784–2790.
- Craft, N.E., and Soares, J.H. (1992). Relative solubility, stability, and absorptivity of lutein and β -carotene in organic-solvents. *J. Agric. Food Chem.* **40**: 431–434.
- De Las Rivas, J., Balsera, M., and Barber, J. (2004). Evolution of oxygenic photosynthesis: Genome-wide analysis of the OEC extrinsic proteins. *Trends Plant Sci.* **9**: 18–25.
- Demmig-Adams, B., and Adams, W.W. (1996). The role of xanthophyll cycle carotenoids in the protection of photosynthesis. *Trends Plant Sci.* **1**: 21–26.
- Eggeling, C., Ringemann, C., Medda, R., Schwarzmann, G., Sandhoff, K., Polyakova, S., Belov, V.N., Hein, B., von Middendorff, C., Schönle, A., and Hell, S.W. (2009). Direct observation of the nanoscale dynamics of membrane lipids in a living cell. *Nature* **457**: 1159–1162.
- Eng, J.K., McCormack, A.L., and Yates III, J.R. (1994). An approach to correlate tandem mass-spectral data of peptides with amino-acid-sequences in a protein database. *J. Am. Soc. Mass Spectrom.* **5**: 976–989.
- Fan, J., Sammalkorpi, M., and Haataja, M. (2010). Formation and regulation of lipid microdomains in cell membranes: Theory, modeling, and speculation. *FEBS Lett.* **584**: 1678–1684.
- Fischer, F., and Poetsch, A. (2006). Protein cleavage strategies for an improved analysis of the membrane proteome. *Proteome Sci.* **4**: 2.
- Fryer, M.J. (1992). The antioxidant effects of thylakoid vitamin E (α -tocopherol). *Plant Cell Environ.* **15**: 381–392.
- Gounaris, K., and Barber, J. (1983). Monogalactosyldiacylglycerol - The most abundant polar lipid in nature. *Trends Biochem. Sci.* **8**: 378–381.
- Grizot, S., and Buchanan, S.K. (2004). Structure of the OmpA-like domain of RmpM from *Neisseria meningitidis*. *Mol. Microbiol.* **51**: 1027–1037.
- Guglielmi, G., Cohen-Bazire, G., and Bryant, D.A. (1981). The structure of *Gloeobacter violaceus* and its phycobilisomes. *Arch. Microbiol.* **129**: 181–189.
- Havaux, M. (1998). Carotenoids as membrane stabilizers in chloroplasts. *Trends Plant Sci.* **3**: 147–151.
- Havaux, M., Tardy, F., Ravenel, J., Chanu, D., and Parot, P. (1996). Thylakoid membrane stability to heat stress studied by flash spectroscopic measurements of the electrochromic shift in intact potato leaves: Influence of the xanthophyll content. *Plant Cell Environ.* **19**: 1359–1368.
- Huang, F., Parmryd, I., Nilsson, F., Persson, A.L., Pakrasi, H.B., Andersson, B., and Norling, B. (2002). Proteomics of *Synechocystis* sp. strain PCC 6803: Identification of plasma membrane proteins. *Mol. Cell. Proteomics* **1**: 956–966.
- Inoue, H., Tsuchiya, T., Satoh, S., Miyashita, H., Kaneko, T., Tabata, S., Tanaka, A., and Mimuro, M. (2004). Unique constitution of photosystem I with a novel subunit in the cyanobacterium *Gloeobacter violaceus* PCC 7421. *FEBS Lett.* **578**: 275–279.
- Iwai, M., Takizawa, K., Tokutsu, R., Okamuro, A., Takahashi, Y., and Minagawa, J. (2010). Isolation of the elusive supercomplex that drives cyclic electron flow in photosynthesis. *Nature* **464**: 1210–1213.
- Jöstingmeyer, P., and Koenig, F. (1998). *Gloeobacter violaceus* - Investigation of carotenoids and carotenoid associated proteins. In *Photosynthesis: Mechanisms and Effects*, G. Garab, ed (Dordrecht, The Netherlands: Kluwer), pp. 229–232.
- Joyard, J., Ferro, M., Masselon, C., Seigneurin-Berny, D., Salvi, D., Garin, J., and Rolland, N. (2009). Chloroplast proteomics and the compartmentation of plastidial isoprenoid biosynthetic pathways. *Mol. Plant* **2**: 1154–1180.
- Jülicher, F., and Lipowsky, R. (1993). Domain-induced budding of vesicles. *Phys. Rev. Lett.* **70**: 2964–2967.
- Kaftan, D., Brumfeld, V., Nevo, R., Scherz, A., and Reich, Z. (2002). From chloroplasts to photosystems: In situ scanning force microscopy on intact thylakoid membranes. *EMBO J.* **21**: 6146–6153.
- Käll, L., Storey, J.D., MacCoss, M.J., and Noble, W.S. (2008). Assigning significance to peptides identified by tandem mass spectrometry using decoy databases. *J. Proteome Res.* **7**: 29–34.
- Kanehisa, M., and Goto, S. (2000). KEGG: Kyoto encyclopedia of genes and genomes. *Nucleic Acids Res.* **28**: 27–30.
- Klinkert, B., Ossenbühl, F., Sikorski, M., Berry, S., Eichacker, L., and Nickelsen, J. (2004). Prata, a periplasmic tetratricopeptide repeat protein involved in biogenesis of photosystem II in *Synechocystis* sp. PCC 6803. *J. Biol. Chem.* **279**: 44639–44644.
- Kouril, R., Arteni, A.A., Lax, J., Yeremenko, N., D'Haene, S., Rögner, M., Matthijs, H.C., Dekker, J.P., and Boekema, E.J. (2005). Structure and functional role of supercomplexes of IsiA and Photosystem I in cyanobacterial photosynthesis. *FEBS Lett.* **579**: 3253–3257.
- Krause, F., Reifschneider, N.H., Vocke, D., Seelert, H., Rexroth, S., and Dencher, N.A. (2004). “Respirasome”-like supercomplexes in green leaf mitochondria of spinach. *J. Biol. Chem.* **279**: 48369–48375.
- Krogmann, D.W., Pérez-Gómez, B., Gutiérrez-Cirlos, E.B., Chagolla-López, A., González de la Vara, L., and Gómez-Lojero, C. (2007). The presence of multidomain linkers determines the bundle-shape structure of the phycobilisome of the cyanobacterium *Gloeobacter violaceus* PCC 7421. *Photosynth. Res.* **93**: 27–43.
- Kyte, J., and Doolittle, R.F. (1982). A simple method for displaying the hydropathic character of a protein. *J. Mol. Biol.* **157**: 105–132.
- Lenn, T., Leake, M.C., and Mullineaux, C.W. (2008a). Are *Escherichia coli* OXPHOS complexes concentrated in specialized zones within the plasma membrane? *Biochem. Soc. Trans.* **36**: 1032–1036.
- Lenn, T., Leake, M.C., and Mullineaux, C.W. (2008b). Clustering and dynamics of cytochrome bd-I complexes in the *Escherichia coli* plasma membrane in vivo. *Mol. Microbiol.* **70**: 1397–1407.
- Lingwood, D., and Simons, K. (2010). Lipid rafts as a membrane-organizing principle. *Science* **327**: 46–50.
- Liu, H., Sadygov, R.G., and Yates III, J.R. (2004). A model for random sampling and estimation of relative protein abundance in shotgun proteomics. *Anal. Chem.* **76**: 4193–4201.
- López, D., and Kolter, R. (2010). Functional microdomains in bacterial membranes. *Genes Dev.* **24**: 1893–1902.
- Mehta, M., Sarafis, V., and Critchley, C. (1999). Thylakoid membrane architecture. *Aust. J. Plant Physiol.* **26**: 709–716.
- Mimuro, M., Tomo, T., and Tsuchiya, T. (2008). Two unique cyanobacteria lead to a traceable approach of the first appearance of oxygenic photosynthesis. *Photosynth. Res.* **97**: 167–176.
- Molitor, V., and Peschek, G.A. (1986). Respiratory electron-transport in plasma and thylakoid membrane preparations from the cyanobacterium *Anacystis nidulans*. *FEBS Lett.* **195**: 145–150.
- Mulkijanian, A.Y., Koonin, E.V., Makarova, K.S., Mekhedov, S.L., Sorokin, A., Wolf, Y.I., Dufresne, A., Partensky, F., Burd, H., Kaznadzey, D., Haselkorn, R., and Galperin, M.Y. (2006). The cyanobacterial genome core and the origin of photosynthesis. *Proc. Natl. Acad. Sci. USA* **103**: 13126–13131.
- Mullineaux, C.W., and Sarcina, M. (2002). Probing the dynamics of photosynthetic membranes with fluorescence recovery after photobleaching. *Trends Plant Sci.* **7**: 237–240.
- Munro, S. (2003). Lipid rafts: Elusive or illusive? *Cell* **115**: 377–388.

- Murata, N., and Omata, T.** (1988). Isolation of cyanobacterial plasma-membranes. *Methods Enzymol.* **167**: 245–251.
- Nakamura, Y., et al.** (2003). Complete genome structure of *Gloeobacter violaceus* PCC 7421, a cyanobacterium that lacks thylakoids. *DNA Res.* **10**: 137–145.
- Nelissen, B., Van de Peer, Y., Wilmotte, A., and De Wachter, R.** (1995). An early origin of plastids within the cyanobacterial divergence is suggested by evolutionary trees based on complete 16S rRNA sequences. *Mol. Biol. Evol.* **12**: 1166–1173.
- Norling, B., Zarka, A., and Boussiba, S.** (1997). Isolation and characterization of plasma membranes from cyanobacteria. *Physiol. Plant.* **99**: 495–504.
- Ohkawa, H., Sonoda, M., Shibata, M., and Ogawa, T.** (2001). Localization of NAD(P)H dehydrogenase in the cyanobacterium *Synechocystis* sp. strain PCC 6803. *J. Bacteriol.* **183**: 4938–4939.
- Omata, T., and Murata, N.** (1983). Isolation and characterization of the cytoplasmic membranes from the blue-green-alga (cyanobacterium) *Anacystis nidulans*. *Plant Cell Physiol.* **24**: 1101–1112.
- Opekarová, M., Malinsky, J., and Tanner, W.** (2010). Plants and fungi in the era of heterogeneous plasma membranes. *Plant Biol. (Stuttg.)* **12** (Suppl. 1): 94–98.
- Parthasarathy, R., Yu, C.H., and Groves, J.T.** (2006). Curvature-modulated phase separation in lipid bilayer membranes. *Langmuir* **22**: 5095–5099.
- Patzlaff, J.S., and Barry, B.A.** (1996). Pigment quantitation and analysis by HPLC reverse phase chromatography: A characterization of antenna size in oxygen-evolving photosystem II preparations from cyanobacteria and plants. *Biochemistry* **35**: 7802–7811.
- Peschek, G.A., Obinger, C., Fromwald, S., and Bergman, B.** (1994). Correlation between immunogold labels and activities of the cytochrome *c* oxidase (*aa₃-tp*) in membranes of salt stressed cyanobacteria. *FEMS Microbiol. Lett.* **124**: 431–438.
- Pisareva, T., Shumskaya, M., Maddalo, G., Ilag, L., and Norling, B.** (2007). Proteomics of *Synechocystis* sp. PCC 6803. Identification of novel integral plasma membrane proteins. *FEBS J.* **274**: 791–804.
- Porra, R.J., Thompson, W.A., and Kriedemann, P.E.** (1989). Determination of accurate extinction coefficients and simultaneous-equations for assaying chlorophyll-*a* and chlorophyll-*b* extracted with 4 different solvents - Verification of the concentration of chlorophyll standards by atomic-absorption spectroscopy. *Biochim. Biophys. Acta* **975**: 384–394.
- Rexroth, S., Meyer zu Tittingdorf, J.M., Krause, F., Dencher, N.A., and Seelert, H.** (2003). Thylakoid membrane at altered metabolic state: challenging the forgotten realms of the proteome. *Electrophoresis* **24**: 2814–2823.
- Rippka, R., Waterbury, J., and Cohen-Bazire, G.** (1974). A cyanobacterium which lacks thylakoids. *Arch. Microbiol.* **100**: 419–436.
- Schägger, H., and Pfeiffer, K.** (2000). Supercomplexes in the respiratory chains of yeast and mammalian mitochondria. *EMBO J.* **19**: 1777–1783.
- Schultze, M., Forberich, B., Rexroth, S., Dyczmons, N.G., Roegner, M., and Appel, J.** (2009). Localization of cytochrome *b₆f* complexes implies an incomplete respiratory chain in cytoplasmic membranes of the cyanobacterium *Synechocystis* sp. PCC 6803. *Biochim. Biophys. Acta* **1787**: 1479–1485.
- Selstam, E., and Campbell, D.** (1996). Membrane lipid composition of the unusual cyanobacterium *Gloeobacter violaceus* sp PCC 7421, which lacks sulfoquinovosyl diacylglycerol. *Arch. Microbiol.* **166**: 132–135.
- Shimoni, E., Rav-Hon, O., Ohad, I., Brumfeld, V., and Reich, Z.** (2005). Three-dimensional organization of higher-plant chloroplast thylakoid membranes revealed by electron tomography. *Plant Cell* **17**: 2580–2586.
- Simons, K., and Ikonen, E.** (1997). Functional rafts in cell membranes. *Nature* **387**: 569–572.
- Staelin, L.A.** (2003). Chloroplast structure: from chlorophyll granules to supra-molecular architecture of thylakoid membranes. *Photosynth. Res.* **76**: 185–196.
- Steiger, S., Jackisch, Y., and Sandmann, G.** (2005). Carotenoid biosynthesis in *Gloeobacter violaceus* PCC4721 involves a single crtI-type phytoene desaturase instead of typical cyanobacterial enzymes. *Arch. Microbiol.* **184**: 207–214.
- Subczynski, W.K., Markowska, E., Gruszecki, W.I., and Siewewiesiuk, J.** (1992). Effects of polar carotenoids on dimyristoylphosphatidylcholine membranes: A spin-label study. *Biochim. Biophys. Acta* **1105**: 97–108.
- Tardy, F., and Havaux, M.** (1997). Thylakoid membrane fluidity and thermostability during the operation of the xanthophyll cycle in higher-plant chloroplasts. *Biochim. Biophys. Acta* **1330**: 179–193.
- Trebst, A., Depka, B., and Holländer-Czytko, H.** (2002). A specific role for tocopherol and of chemical singlet oxygen quenchers in the maintenance of photosystem II structure and function in *Chlamydomonas reinhardtii*. *FEBS Lett.* **516**: 156–160.
- Tsuchiya, T., Takaichi, S., Misawa, N., Maoka, T., Miyashita, H., and Mimuro, M.** (2005). The cyanobacterium *Gloeobacter violaceus* PCC 7421 uses bacterial-type phytoene desaturase in carotenoid biosynthesis. *FEBS Lett.* **579**: 2125–2129.
- Usaitė, R., Wohlschlegel, J., Venable, J.D., Park, S.K., Nielsen, J., Olsson, L., and Yates III, J.R.** (2008). Characterization of global yeast quantitative proteome data generated from the wild-type and glucose repression *saccharomyces cerevisiae* strains: The comparison of two quantitative methods. *J. Proteome Res.* **7**: 266–275.
- van de Meene, A.M.L., Hohmann-Marriott, M.F., Vermaas, W.F.J., and Roberson, R.W.** (2006). The three-dimensional structure of the cyanobacterium *Synechocystis* sp. PCC 6803. *Arch. Microbiol.* **184**: 259–270.
- Welti, R., Li, W., Li, M., Sang, Y., Biesiada, H., Zhou, H.E., Rajashekar, C.B., Williams, T.D., and Wang, X.** (2002). Profiling membrane lipids in plant stress responses. Role of phospholipase D alpha in freezing-induced lipid changes in Arabidopsis. *J. Biol. Chem.* **277**: 31994–32002.
- Welti, R., Wang, X., and Williams, T.D.** (2003). Electrospray ionization tandem mass spectrometry scan modes for plant chloroplast lipids. *Anal. Biochem.* **314**: 149–152.
- Yokthongwattana, K., Savchenko, T., Polle, J.E.W., and Melis, A.** (2005). Isolation and characterization of a xanthophyll-rich fraction from the thylakoid membrane of *Dunaliella salina* (green algae). *Photochem. Photobiol. Sci.* **4**: 1028–1034.
- Zak, E., Norling, B., Maitra, R., Huang, F., Andersson, B., and Pakrasi, H.B.** (2001). The initial steps of biogenesis of cyanobacterial photosystems occur in plasma membranes. *Proc. Natl. Acad. Sci. USA* **98**: 13443–13448.
- Zhang, P., Battchikova, N., Jansen, T., Appel, J., Ogawa, T., and Aro, E.M.** (2004). Expression and functional roles of the two distinct NDH-1 complexes and the carbon acquisition complex NdhD3/NdhF3/CupA/SII1735 in *Synechocystis* sp PCC 6803. *Plant Cell* **16**: 3326–3340.
- Zhang, Y., Wen, Z., Washburn, M.P., and Florens, L.** (2009). Effect of dynamic exclusion duration on spectral count based quantitative proteomics. *Anal. Chem.* **81**: 6317–6326.
- Zybailov, B., Mosley, A.L., Sardi, M.E., Coleman, M.K., Florens, L., and Washburn, M.P.** (2006). Statistical analysis of membrane proteome expression changes in *Saccharomyces cerevisiae*. *J. Proteome Res.* **5**: 2339–2347.
- Zybailov, B., Rutschow, H., Friso, G., Rudella, A., Emanuelsson, O., Sun, Q., and van Wijk, K.J.** (2008). Sorting signals, N-terminal modifications and abundance of the chloroplast proteome. *PLoS One* **3**: e1994.

The Plasma Membrane of the Cyanobacterium *Gloeobacter violaceus* Contains Segregated Bioenergetic Domains

Sascha Rexroth, Conrad W. Mullineaux, Dorothea Ellinger, Esther Sendtko, Matthias Rögner and Friederike Koenig

Plant Cell 2011;23;2379-2390; originally published online June 3, 2011;
DOI 10.1105/tpc.111.085779

This information is current as of August 22, 2011

Supplemental Data	http://www.plantcell.org/content/suppl/2011/05/18/tpc.111.085779.DC1.html
References	This article cites 79 articles, 16 of which can be accessed free at: http://www.plantcell.org/content/23/6/2379.full.html#ref-list-1
Permissions	https://www.copyright.com/ccc/openurl.do?sid=pd_hw1532298X&issn=1532298X&WT.mc_id=pd_hw1532298X
eTOCs	Sign up for eTOCs at: http://www.plantcell.org/cgi/alerts/ctmain
CiteTrack Alerts	Sign up for CiteTrack Alerts at: http://www.plantcell.org/cgi/alerts/ctmain
Subscription Information	Subscription Information for <i>The Plant Cell</i> and <i>Plant Physiology</i> is available at: http://www.aspb.org/publications/subscriptions.cfm